AMERICAN SOCIETY FOR MICROBIOLOGY | mBio®

RESEARCH ARTICLE

Conductive Particles Enable Syntrophic Acetate Oxidation between *Geobacter* and *Methanosarcina* from Coastal Sediments

Amelia-Elena Rotaru,[a] Federica Calabrese,[b] Hryhoriy Stryhanyuk,[b] Florin Musat,[b] Pravin Malla Shrestha,[c] Hannah Sophia Weber,[a] Oona L. O. Snoeyenbos-West,[a] Per O. J. Hall,[d] Hans H. Richnow,[b] Niculina Musat,[b] Bo Thamdrup[a]

[a]Department of Biology, University of Southern Denmark, Odense, Denmark
[b]Helmholtz Centre for Environmental Research, Leipzig, Germany
[c]Energy Bioscience Institute, University of California Berkeley, Berkeley, USA
[d]Department of Marine Sciences, University of Gothenburg, Gothenburg, Sweden

ABSTRACT Coastal sediments are rich in conductive particles, possibly affecting microbial processes for which acetate is a central intermediate. In the methanogenic zone, acetate is consumed by methanogens and/or syntrophic acetate-oxidizing (SAO) consortia. SAO consortia live under extreme thermodynamic pressure, and their survival depends on successful partnership. Here, we demonstrate that conductive particles enable the partnership between SAO bacteria (i.e., *Geobacter* spp.) and methanogens (*Methanosarcina* spp.) from the coastal sediments of the Bothnian Bay of the Baltic Sea. Baltic methanogenic sediments were rich in conductive minerals, had an apparent isotopic fractionation characteristic of CO_2-reductive methanogenesis, and were inhabited by *Geobacter* and *Methanosarcina*. As long as conductive particles were delivered, *Geobacter* and *Methanosarcina* persisted, whereas exclusion of conductive particles led to the extinction of *Geobacter*. Baltic *Geobacter* did not establish a direct electric contact with *Methanosarcina*, necessitating conductive particles as electrical conduits. Within SAO consortia, *Geobacter* was an efficient [^{13}C]acetate utilizer, accounting for 82% of the assimilation and 27% of the breakdown of acetate. *Geobacter* benefits from the association with the methanogen, because in the absence of an electron acceptor it can use *Methanosarcina* as a terminal electron sink. Consequently, inhibition of methanogenesis constrained the SAO activity of *Geobacter* as well. A potential benefit for *Methanosarcina* partnering with *Geobacter* is that together they competitively exclude acetoclastic methanogens like *Methanothrix* from an environment rich in conductive particles. Conductive particle-mediated SAO could explain the abundance of acetate oxidizers like *Geobacter* in the methanogenic zone of sediments where no electron acceptors other than CO_2 are available.

IMPORTANCE Acetate-oxidizing bacteria are known to thrive in mutualistic consortia in which H_2 or formate is shuttled to a methane-producing *Archaea* partner. Here, we discovered that such bacteria could instead transfer electrons via conductive minerals. Mineral SAO (syntrophic acetate oxidation) could be a vital pathway for CO_2-reductive methanogenesis in the environment, especially in sediments rich in conductive minerals. Mineral-facilitated SAO is therefore of potential importance for both iron and methane cycles in sediments and soils. Additionally, our observations imply that agricultural runoff or amendments with conductive chars could trigger a significant increase in methane emissions.

KEYWORDS *Desulfuromonadales*, *Geobacter*, *Methanosarcina*, nanoSIMS, activated carbon, competitive exclusion, direct interspecies electron transfer, syntrophic acetate oxidation

Received 28 January 2018 **Accepted** 28 March 2018 **Published** 1 May 2018

Citation Rotaru A-E, Calabrese F, Stryhanyuk H, Musat F, Shrestha PM, Weber HS, Snoeyenbos-West OLO, Hall POJ, Richnow HH, Musat N, Thamdrup B. 2018. Conductive particles enable syntrophic acetate oxidation between *Geobacter* and *Methanosarcina* from coastal sediments. mBio 9:e00226-18. https://doi.org/10.1128/mBio.00226-18.

Editor Stephen J. Giovannoni, Oregon State University

Address correspondence to Amelia-Elena Rotaru, arotaru@biology.sdu.dk, or Niculina Musat, niculina.musat@ufz.de.

Syntrophic acetate-oxidizing (SAO) bacteria live in a mutualistic interaction with methanogenic archaea, which feed on the H_2 or formate released by the SAO bacterial partner (1). Besides H_2 or formate, cysteine can also be used to transfer electrons in some SAO consortia (2). Several studies with synthetic consortia have shown SAO activity in members of the phyla *Firmicutes* (*Thermacetogenium*, *Clostridium*, *Thermotoga*, *Candidatus* Contubernalis, and *Syntrophaceticus*) and *Proteobacteria* (*Desulfomicrobium* and *Geobacter*) (2–14). Remarkably, acetoclastic methanogens (*Methanosarcina* and *Methanothrix*) have been proposed to play the role of syntrophic acetate oxidizers when provided with an appropriate H_2-consuming partner (15, 16). Some of the genera above have been suggested to carry out SAO in thermophilic digesters (17–26), lake/river sediments (21, 27, 28), tropical wetland soil (29), rice paddies (30–32), or oil field reservoirs (33). Many of these environments are rich in (semi)conductive minerals like magnetite (34, 35), pyrite (36, 37), or black carbon resulting from incomplete burning of plant biomass (38–40). Electrically conductive iron oxide minerals and carbon chars (magnetite, granular activated carbon, biochar) were previously shown to stimulate direct interspecies electron transfer (DIET), a recently described form of interspecies electron transfer (12, 41–49), whereas strict H_2-based interactions were shown to remain unaffected by the addition of conductive materials (44). DIET is a syntrophic association where electrons are transferred via conductive and/or redox-active cell surface structures between an electron-donating species (electrogen) and an electron-accepting species (electrotroph) (47–49). Conductive minerals seem to alleviate the need for cells to produce certain cell surface molecules required for DIET (41). DIET mediated by conductive materials is considered a novel strategy to stimulate recalcitrant organic matter decomposition in anaerobic digesters (50–52) and to enhance methanogenic decomposition of organics in rice paddies (46, 53) and aquatic sediments (28, 54). It is likely that conductive materials replace the molecular conduits that cells require to establish direct contacts during DIET.

Although SAO via DIET is considered thermodynamically favorable at pH values between 1.9 and 2.9 and impossible at pH 7 (55), conductive minerals have been shown to facilitate SAO in synthetic denitrifying consortia at pH 7 (56). Nevertheless, the impact of minerals on environmentally relevant SAO is presently not understood. Mineral-facilitated SAO (here called mineral-SAO) could be significant in coastal environments rich in (semi)conductive minerals (36, 57–59). Such (semi)conductive minerals are likely to impact microbial processes (36, 56), for which acetate is a central intermediate (88–90).

Here, we investigated the role of mineral-SAO in methanogenic processes from coastal sediments. We examined if electrically conductive materials mediate SAO between *Geobacter* and *Methanosarcina* organisms coexisting in the brackish, iron-rich coastal sediments of Bothnian Bay. Our results indicate that mineral-SAO may impact both the iron and the methane cycles in these sediments, with implications for atmospheric methane emissions.

RESULTS AND DISCUSSION

In this study, we found that methanogenic communities from Bothnian Bay made use of (semi)conductive particles to facilitate SAO. For this, we used a combination of physiological and stable isotope labeling experiments followed by monitoring of labeled products and incorporation of the labeled substrate in phylogenetically assigned cells by using nanoscale secondary ion mass spectrometry (nanoSIMS) coupled with catalyzed reporter deposition fluorescent *in situ* hybridization (CARD-FISH).

Syntrophic acetate oxidizers are difficult to enrich (57), because SAO is thermodynamically challenging (55). Here, we successfully enriched SAO consortia from temperate sediments (sediment temperature, 15°C; incubation temperature, 20 to 25°C) by successive cultivation in the presence of electrically conductive (>1,000 S/m [58]) granular activated carbon (GAC).

Characteristics of the Bothnian Bay methanogenic zone. (i) Geochemistry. Our hypothesis was that a high conductive mineral content would stimulate electric

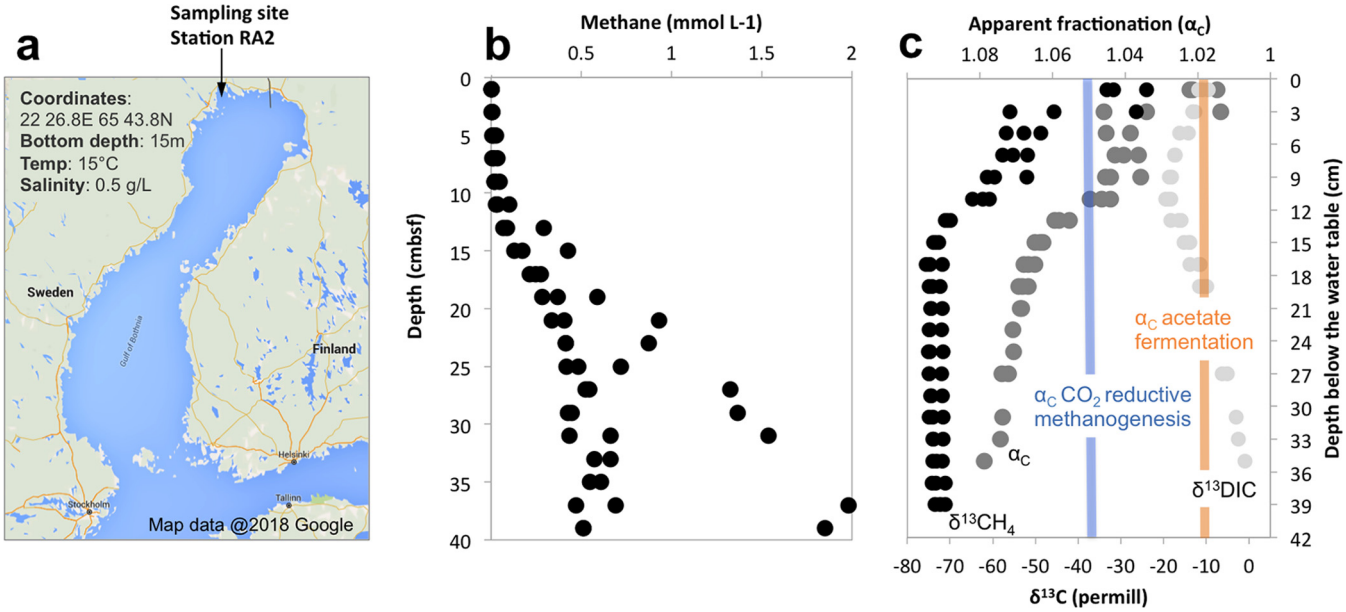

FIG 1 CO_2-reductive methanogenesis in the Bothnian Bay methanogenic zone. (a) The sampling site, RA2, was located off the Bothnian Bay northern coast. (b and c) Here, methane accumulated close to and sometimes over the saturation limit (b) and was strongly depleted in ^{13}C (low $\delta^{13}CH_4$), which indicated a high apparent fractionation (α_C) characteristic of CO_2-reductive methanogenesis (c). Previous studies showed an α_C of ca. 1.05 (blue line) in *Methanosarcina* grown via CO_2-reductive methanogenesis (85, 86). An α_C of ca. 1.02 (orange line) was observed in *Methanosarcina* species grown by acetoclastic methanogenesis (87).

interactions between abundant electroactive microorganisms coexisting in the methanogenic zone. The Bothnian Bay sediments are rich in conductive minerals dispersed either within the fine structure of sediments or within ferromanganese nodules (59).

To explore mineral-mediated interactions in Bothnian Bay, we sampled the methanogenic zone of these sediments to verify the mineral content. Sediment cores were collected from 15-m water depth at station RA2, located at 65°43.6′N and 22°26.8′E in Bothnian Bay (Fig. 1), which had high sediment temperature (15°C) and low *in situ* salinity (0.5). The mineral content was low in manganese oxides (13 ± 3 μmol/cm^3 [mean ± standard deviation] from both HCl and dithionite extractions), high in FeS, $FeCO_3$, and other poorly crystalline Fe-minerals (229 ± 8 μmol/cm^3), and high in crystalline iron oxides (dithionite-extractable iron, 131 ± 4 μmol/cm^3) and conductive magnetite (32 ± 7 μmol/cm^3 oxalate extractable). This estimate of the magnetite content was similar to what has been previously observed below the sulfate-methane transition zone in Baltic Sea sediments (ca. 30 μmol/cm^3) (60).

Besides iron oxide minerals, previous studies showed that black carbon, also a conductive material (40), dominated the coastal sediments of the Baltic Sea, representing 1.7% to 46% of the total organic carbon (TOC) in sediments closer to coastal towns (61). Conductive materials could reach Bothnian Bay by river runoff from the eight rivers entering the bay from Sweden and Finland, and also via runoff from the forestry industry and various coastal industries (59, 62).

The high abundance of conductive particles likely stimulates electrical interactions between abundant electroactive microorganisms that coexist in the methanogenic zone (41–43, 45, 52). Methane reached its highest concentrations below 25 cm depth (Fig. 1). In the methanogenic zone, two independent processes, SAO and/or acetoclastic methanogenesis, could consume acetate, a key intermediate of organic matter decomposition. SAO bacteria would need a CO_2-reductive methanogenic partner to scavenge the electrons released during acetate oxidation. To find out if CO_2-reductive methanogenesis was occurring in these sediments, we looked at the apparent isotopic fractionation of dissolved organic carbon (DIC, which includes CO_2, carbonic acid, bicarbonate, and carbonate) and methane. Methane was strongly depleted in ^{13}C relative to DIC

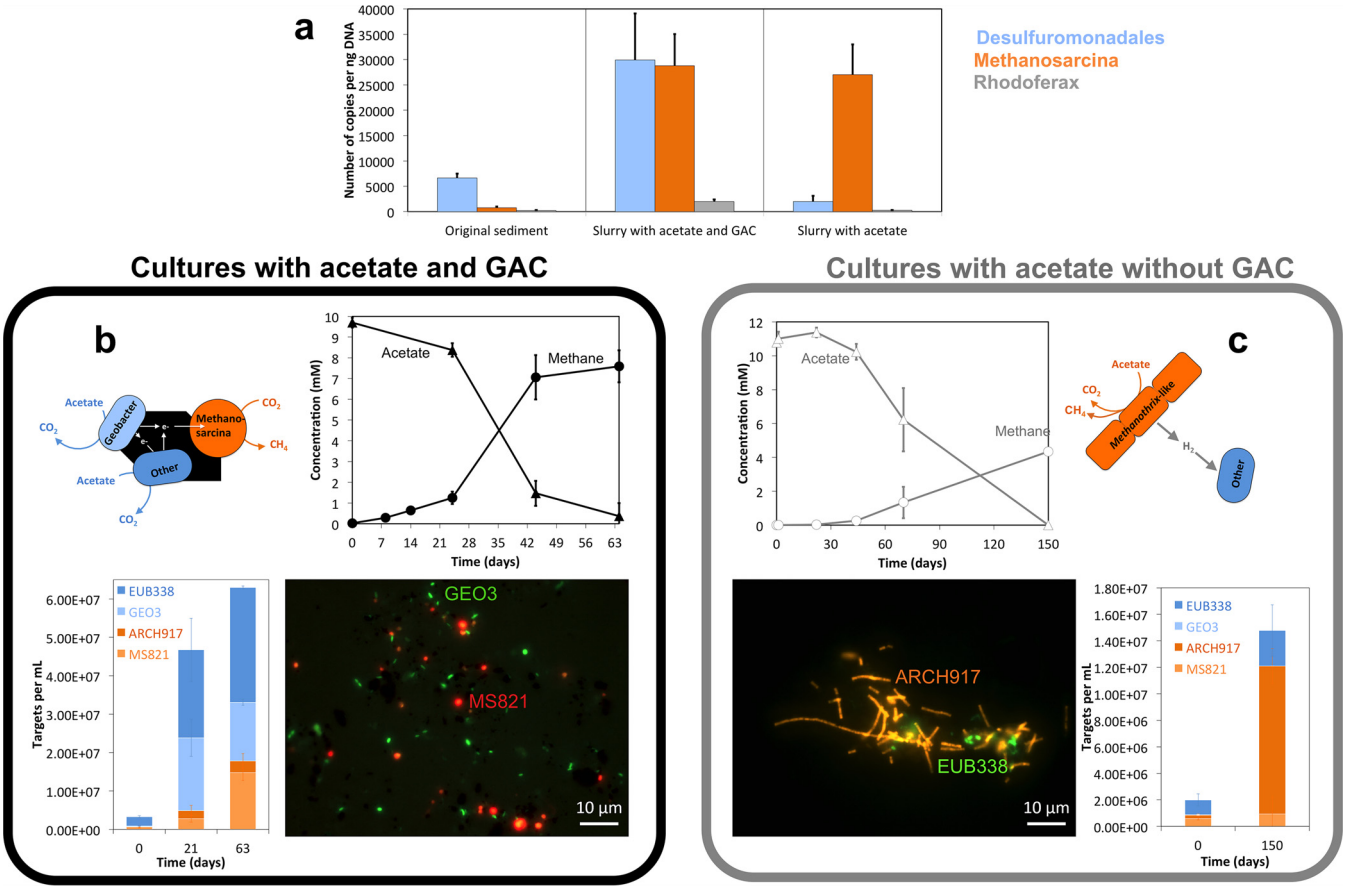

FIG 2 Incubation mixtures with and without activated carbon and representative organisms. (a) Quantitative PCR in original sediment samples showed that *Desulfuromonadales* were the dominant electrogens in the original sediment and in sediment slurries with conductive particles, but this group was almost extinct in a first slurry transfer without conductive particles. The only methanogens detected by qPCR in the original sediments were DIET-associated *Methanosarcina*, which remained abundant in slurry incubation mixtures with or without conductive particles. (b) In mud-free incubation mixtures with conductive GAC (sixth consecutive mud-free transfer), acetate was completely depleted after 63 days, and it was converted to methane with a high stoichiometric recovery (82%). *Methanosarcina* was the only *Archaea* genus detected in these mud-free cultures. Together, *Methanosarcina* and *Geobacter* represented ca. half of the microbial community, as determined by CARD-FISH. (c) On the other hand, in control incubation mixtures without conductive materials (third consecutive mud-free transfer), acetate consumption was much slower. Acetate was depleted after 150 days and converted to methane, with only 40% stoichiometric recovery. In control incubation mixtures without conductive GAC, *Geobacter* and *Methanosarcina* were led to extinction (Fig. S5F). Instead *Methanothrix*-like filamentous *Archaea* carried acetate utilization in control incubation mixtures without GAC (Fig. S5F).

(median $\delta^{13}CH_4$, −74‰, median $\delta^{13}DIC$, −2.5‰) (Fig. 1), which resulted in a signature apparent isotopic fractionation (α_c) of 1.07, characteristic of CO_2-reductive methanogenesis (63).

(ii) Microbial community. DIET consortia (*Geobacter* and *Methanosarcina*) can usually form more efficient electron transfer associations via conductive minerals than they do in their absence (42–44, 64). In contrast, H_2-transferring consortia have been shown to remain little affected by conductive materials (44, 65). We predicted that Bothnian Bay sediments rich in conductive minerals are favorable for mineral DIET associations. As anticipated, these iron mineral-rich sediments harbored *Proteobacteria*, including exo-electrogens related to *Geobacter* and *Rhodoferax*, and *Archaea* methanogens related to *Methanosarcina* (Fig. 2a; see also Fig. S2F). Both *Geobacter* and *Rhodoferax* were previously shown to form DIET associations with species of Methanosarcinales (48, 64; A.-E. Rotaru and D. R. Lovley, unpublished data). Until now, only Methanosarcinales were shown to establish DIET associations with electrogens (48, 49, 64), probably due to their high *c*-type cytochrome content, which allows for electron uptake from electrogens (48, 66).

Based on the observations that (i) sediments were high in conductive mineral content, (ii) CO_2-reductive methanogenesis prevailed, and (iii) *Methanosarcina* and

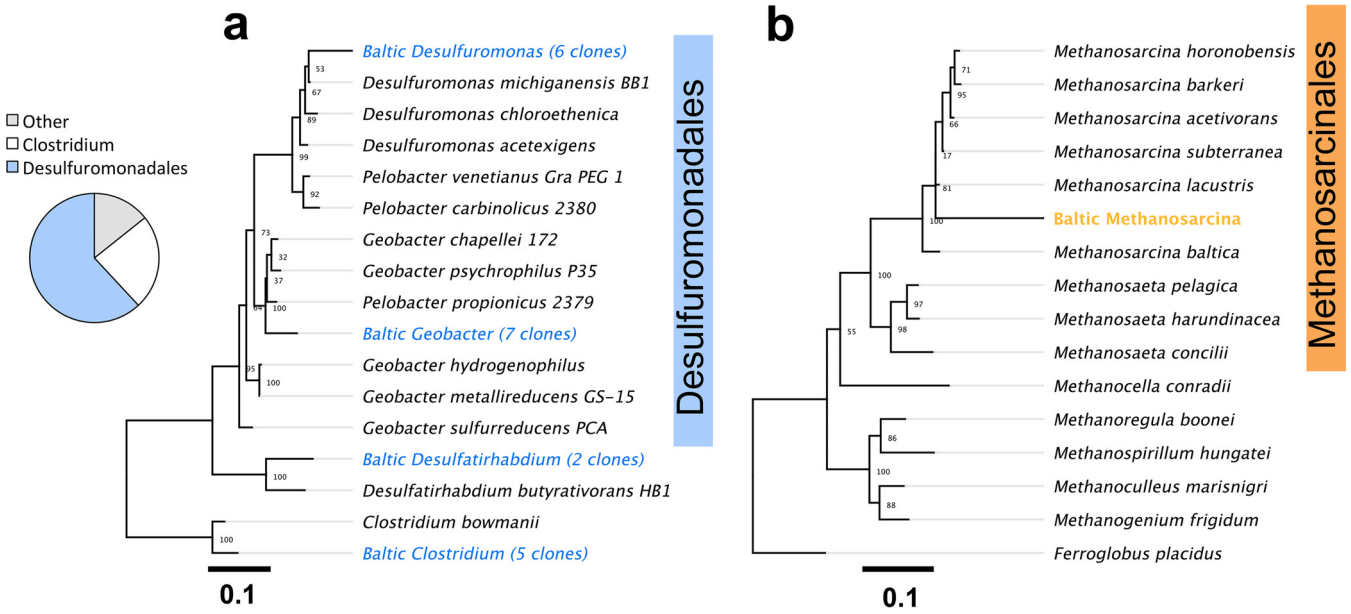

FIG 3 Maximum likelihood trees of *Bacteria* and *Archaea* enriched in a seventh mud-free transfer with acetate and GAC. (a) A maximum likelihood tree of representative bacterial sequences from a mud-free transfer with conductive particles (GAC), under conditions strictly promoting methanogenic respiration. Acetate-oxidizing *Desulfuromonadales* dominated the 16S rRNA clone library, with more than half displaying close relationships to *Geobacter psychrophilus* (97% identity) and the rest to *Desulfuromonas michiganensis* (98%). The only methanogens enriched on acetate and GAC were relatives of *Methanosarcina subterranea* (99% identity), as shown in the maximum likelihood tree in panel b.

electrogens cohabited, we anticipated that mineral DIET could occur in the methanogenic zone of Bothnian Bay. We tested this hypothesis in sediment incubations with or without the addition of exogenous conductive particles.

Conductive GAC facilitated methane production from acetate (Fig. 2) and other substrates (ethanol, butyrate, and glucose) that were degraded via acetate (Fig. S3F). Tests with conductive magnetite showed that it stimulated methanogenesis even more than GAC (Fig. S4F). On the other hand, nonconductive glass beads did not facilitate methanogenesis from ethanol (Fig. 3SF), as these mixtures produced as much methane as incubation mixtures without GAC ($P = 0.45$). However, GAC was the preferred conductive particle, because we could concentrate rigorously on electron transfer (42), whereas with use of (semi)conductive magnetite ($Fe^{II}Fe^{III}_2O_4$) its Fe^{III} content could additionally drive iron reduction, especially during long-term incubations (67, 68).

Syntrophic acetate oxidation mediated by GAC. Repeated transfers of the SAO cultures with acetate as electron donor, CO_2 as electron acceptor, and GAC produced methane much faster than GAC-free controls and led to sediment-free cultures enriched in *Desulfuromonadales* (*Geobacter* and *Desulfuromonas*) and *Methanosarcina* (Fig. 2). The enriched *Desulfuromonadales* were related to acetate oxidizers like *G. psychrophilus* with (97% sequence identity) and *D. michiganensis* (98% sequence identity) (Fig. 3). The only methanogens detected in mud-free enrichments were related to *Methanosarcina subterranea* (99% sequence identity) (Fig. 3). In the absence of conductive minerals, *Geobacter* and *Methanosarcina* became undetectable after several mud-free transfers (Fig. 2), and a filamentous *Archaea* (a *Methanothrix*-like morphotype) took over acetate-only incubation mixtures (Fig. 2; Fig. S5F).

In incubation mixtures with acetate and GAC, acetate could be consumed by acetoclastic methanogens and/or SAO consortia. A schematic representation of SAO mediated by GAC tied to methanogenesis is presented in Fig. 4. Our hypothesis was that during SAO, *Geobacter* cells donate electrons from the oxidation of acetate to GAC, which then plays the role of a transient electron acceptor. Then, *Methanosarcina* cells retrieve the electrons from GAC in order to reduce CO_2 to methane.

To distinguish between acetoclastic methanogenesis and SAO, cultures were incubated with $^{13}CH_3{}^{12}COOH$. If acetoclastic methanogens utilized the [^{13}C]methyl on

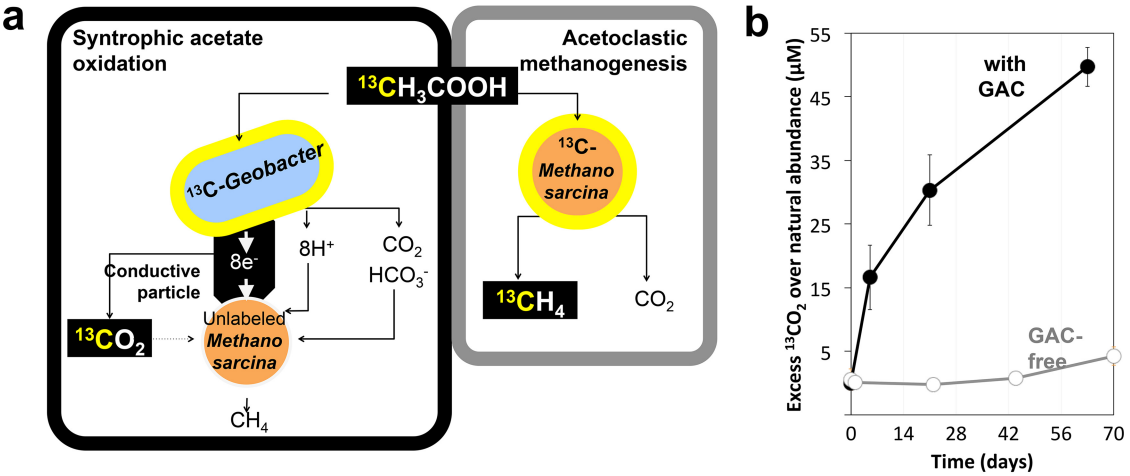

c

^{13}C-label	Day 0**	Day 21**	Day 63***
$^{13}CH_3{}^{12}COOH$ acetate* (µM)	980 ± 33	821 ± 66	181 ± 23
Consumed $^{13}CH_3{}^{12}COOH$ acetate* (µM)	-	159 ± 37	640 ± 35
$^{13}CO_2$ (µM detected in solution and equilibrated with headspace)	0 ± 0	43 ± 3	67 ± 1
Estimated ^{13}C-respiration (%) by SAO	NA	27.0%	8.4%
Estimated ^{13}C-respiration (%) by acetoclastic *Methanosarcina*	NA	27.4%	61.8%

*10% of the acetate added was $^{13}CH_3{}^{12}COOH$, the rest is unlabeled acetate.

**Values are replicate of 4 independent sacrificial cultures

***Values are replicate of 2 independent sacrificial cultures

NA=not applicable

FIG 4 Experimental approach and evidence for SAO. (a) Experimental approach to distinguish between SAO and acetoclastic methanogenesis based on isotopic labeling. $^{13}CH_3{}^{12}COOH$ was provided as 10% of the total acetate, which played the role of the electron donor for SAO consortia from the Bothnian Bay. During SAO, acetate-oxidizing *Geobacter* cells are expected to produce $^{13}CO_2$ (^{13}C, depicted in orange) and to incorporate [^{13}C]acetate. During SAO, $^{13}CO_2$ will be diluted by the bicarbonate in the medium and should not generate significant $^{13}CH_4$. However, acetoclastic methanogenesis by *Methanosarcina* cells will generate $^{13}CH_4$ from $^{13}CH_3{}^{12}COOH$, while cells incorporate [^{13}C]acetate in their cell mass. Cells expected to incorporate [^{13}C]acetate are encircled in orange. (b) SAO activity was validated by using labeled $^{13}CO_2$ production from acetate, especially in SAO consortia provided with GAC (blue) versus cultures without GAC (orange). (c) An overview of acetate catabolism and how much is used for respiration by *Geobacter* versus acetoclastic methanogenesis by *Methanosarcina*.

acetate, they would only produce $^{13}CH_4$. However, if SAO bacteria utilized [^{13}C]acetate, then they would produce $^{13}CO_2$ (Fig. 4). When acetoclastic methanogens and SAO bacteria use [^{13}C]methyl on acetate at the same time, both $^{136}CO_2$ and $^{13}CH_4$ would be produced. Our results support the latter model.

(i) SAO dependency on GAC. Incubations for ca. 70 days with [^{13}C]acetate and GAC converted the [^{13}C]methyl on acetate to $^{13}CO_2$, whereas control cultures lacking GAC produced little $^{13}CO_2$ (Fig. 4). This indicated that indeed GAC stimulated SAO.

(ii) Respiratory metabolism and SAO. During exponential growth (day 21), SAO could explain 27% of the total respiratory metabolism, whereas 27.4% could be explained by acetoclastic methanogenesis (Fig. 4). During stationary phase (day 63), SAO justified 8.4% of the total respiratory metabolism, whereas acetoclastic methanogenesis justified 61.8%.

(iii) Biosynthetic metabolism and SAO. The increase in abundance of *Geobacter* cells over time (Fig. 2) in incubation mixtures with GAC indicated that they could play the role of syntrophic acetate oxidizers in mineral-mediated SAO syntrophy. This was confirmed by analysis of the $^{13}CH_3{}^{12}COOH$-incubated SAO consortia by using nanoSIMS/CARD-FISH, an approach that helps correlate phylogeny and function (78). During incubation with GAC, both *Geobacter* and *Methanosarcina* cells became greatly

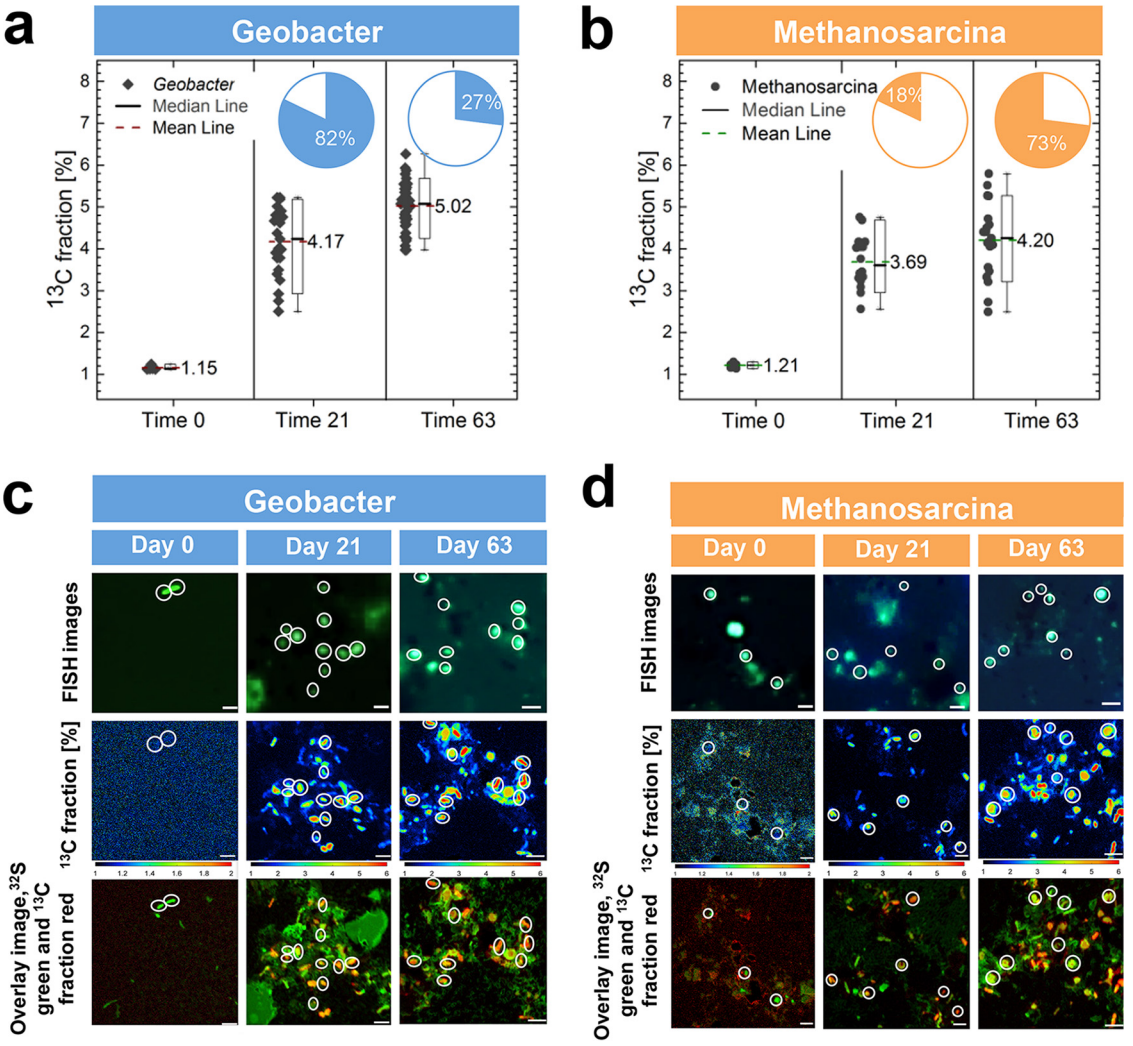

FIG 5 nanoSIMS identification of cells incorporating ^{13}C-labeled acetate. (a and b) Highly abundant *Geobacter* cells (a) incorporated more $^{13}CH_3{}^{12}COOH$ per cell than *Methanosarcina* (b). Insets for panels a and b show percent assimilation in *Geobacter* (blue insets) and *Methanosarcina* (orange) over time. (c) Time-dependent distribution of cells labeled by *Geobacter*-specific probes compared with time-dependent incorporation of $^{13}CH_3COOH$ in *Geobacter* cells (see scales below images) and an overlay of ^{13}C incorporation (red) to total biomass as detected by tracing ^{32}S (green), using nanoSIMS. (d) Time-dependent distribution of cells labeled by *Methanosarcina*-specific probes compared with time-dependent incorporation of $^{13}CH_3COOH$ in *Methanosarcina*-cells (see scales below images) and an overlay of ^{13}C incorporation (red) to total biomass as detected by tracing ^{32}S (green) using nanoSIMS.

enriched in ^{13}C, indicating label assimilation from acetate (Fig. 5a and b). During exponential phase (day 21 *Geobacter* cells were 6 times more abundant than *Methanosarcina*) (Fig. 2). Therefore, the entire *Geobacter* population assimilated 5 times more acetate than the *Methanosarcina* population (Fig. 5). However, upon prolonged incubation (day 63), the number of *Geobacter* cells remained relatively constant, while *Methanosarcina* cells increased in abundance to match the *Geobacter* population (Fig. 2). As a consequence, during the late incubation phase, the *Methanosarcina* population assimilated 3-fold more acetate than *Geobacter* (Fig. 5).

The ratio of *Geobacter* to *Methanosarcina* cells in the original sediment (8:1) was more similar to that observed in incubation during exponential growth (6:1) than to that observed during stationary phase (1:1). During exponential growth, *Geobacter* cells incorporate a high amount of ^{13}C label. Although nanoSIMS results indicated that *Geobacter* could be the primary acetate oxidizer in SAO consortia from the Baltic Sea (Fig. 5), *Desulfuromonas* might also play a significant role in the process.

(iv) SAO is coupled to methanogenesis via a conductive particle electron conduit. To verify if *Methanosarcina* was used as a terminal electron acceptor by the

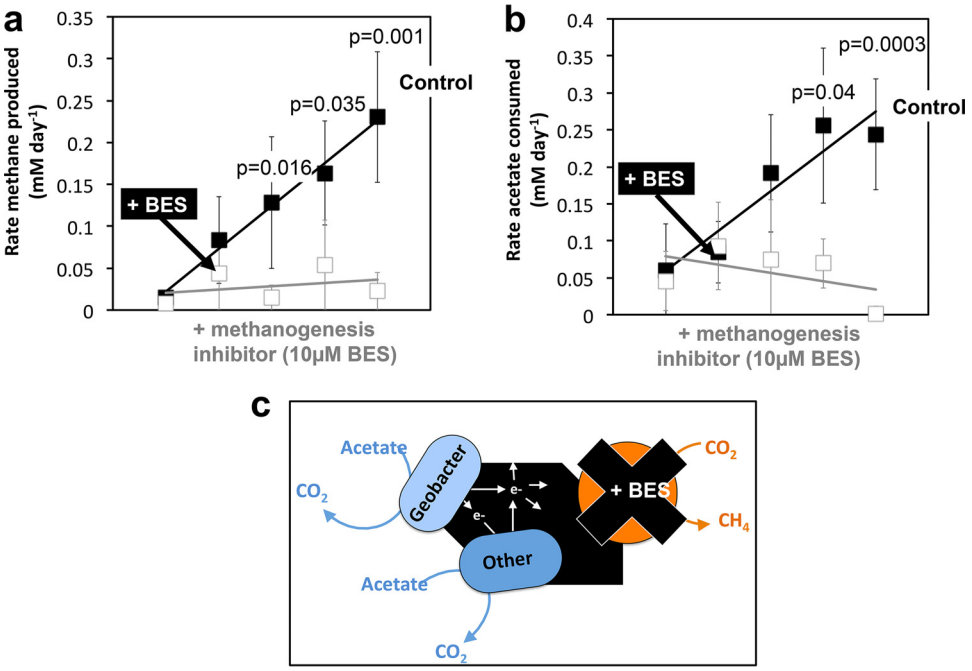

FIG 6 Syntrophic acetate-oxidizing bacteria cannot grow alone on acetate and GAC; they require the methanogen. If conductive GAC were sufficient for SAO bacteria to carry out acetate oxidation, the methanogenic inhibitor bromoethane sulfonate (BES) would collapse the rates of both methanogenesis (a) and acetate oxidation (b), indicating that the two processes are coupled and that *Geobacter* cannot grow alone on acetate and GAC. Methane production (a) and acetate utilization (b) rates were measured in cultures spiked with BES, in contrast to controls lacking BES and (c) a simplified representation of the BES inhibition effect on methanogenesis.

acetate oxidizers, we chemically inhibited the metabolic activity of the methanogen by using a methyl-coenzyme M analogue (10 μM 2-bromoethanesulfonate [BES]) (69). If the acetate oxidizers were able to respire GAC, independent of electron uptake by *Methanosarcina*, we should be able to decouple acetate utilization from methanogenesis. However, acetate utilization ceased as soon as methanogenesis was inhibited by BES (Fig. 6), indicating that the (exo)electrogenic syntrophic acetate oxidizer (*Geobacter*) used the *Methanosarcina* methanogen as an electron sink. *Geobacter*'s dependency on the methanogen could be explained either by an interspecies interaction mediated by GAC (42, 48, 64) or a direct association based on self-assembled molecular conduits on the surface of the cells (48, 49, 70). To resolve if cells adapted to carry a DIET type of interaction via redox-active surface conduits, we switched the highly enriched *Geobacter-Methanosarcina* consortia to a medium without conductive particles. Only *Methanosarcina* survived the change (Fig. 7; Fig. S5F), demonstrating that without a conductive surface, Baltic *Geobacter* could not forge connections with the methanogen on its own. This is in contrast with previous studies on synthetic *Geobacter-Methanosarcina* consortia (48, 64). *Geobacter*'s inability to establish an interspecies interaction with the methanogen in the absence of conductive particles suggests that *Geobacter* used the conductive particle as an electron conduit for extracellular electron transfer and *Methanosarcina* as an electron sink. In what way *Geobacter* releases electrons extracellularly onto GAC and in what way *Methanosarcina*, but not *Methanothrix*, retrieves electrons from GAC are yet unresolved. Nevertheless, the ability of *Methanosarcina* to interact with *Geobacter* via conductive particles would likely give this methanogen a competitive advantage over *Methanothrix* in mineral-rich environments like the Baltic Sea.

(v) Exoenzymes and shuttles are not endogenously created. Previous studies indicated that extracellular enzymes could act as manufacturers of diffusible chemicals (H_2, formate) which could be used for electron transfer to methanogens (71). To test this hypothesis, we spiked cultures with spent medium from a fully grown culture that

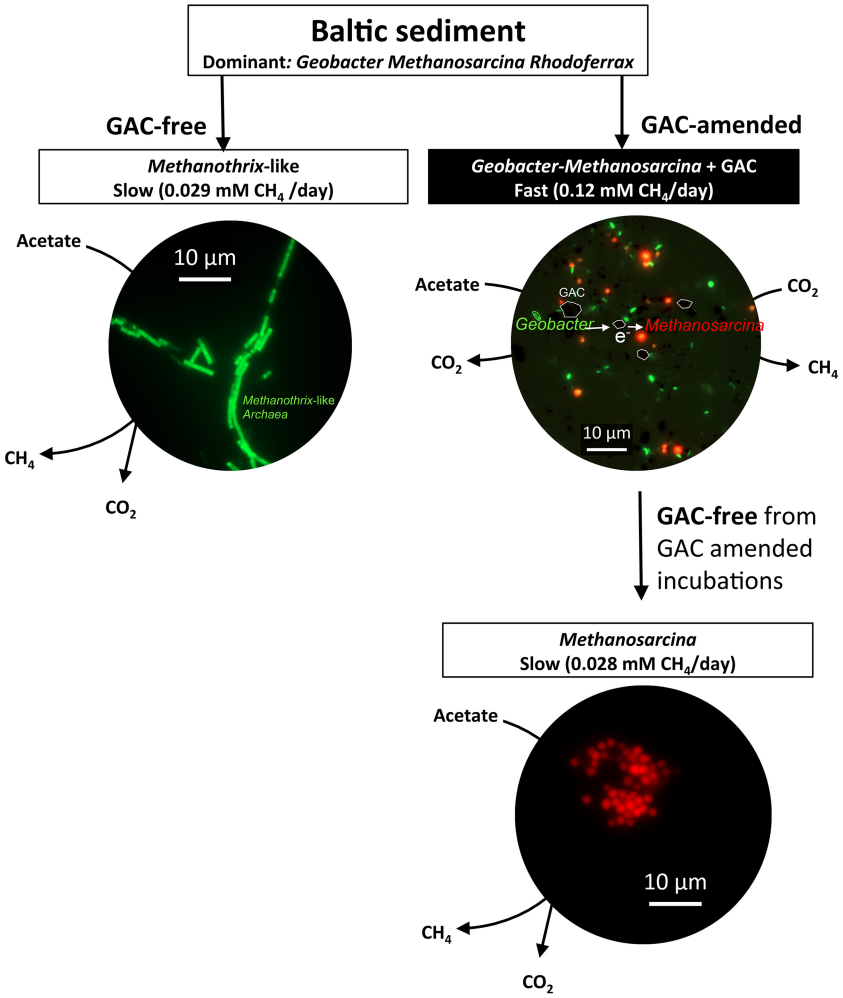

FIG 7 Model interactions with different treatments of a Baltic methanogenic community. *Geobacter* (green) and *Methanosarcina* (red) consortia competitively displaced *Methanothrix*-like (green) cells in Baltic sediments rich in iron-oxide minerals and in conductive particle-amended incubation mixtures. *Geobacter* was only present in incubation mixtures with conductive particles (Fig. S5F).

was filtered through a 0.2-μm filter. The spent medium should theoretically contain (exo)cellular enzymes or potential shuttles, and if these were involved in electron transfer between the microorganisms from the Bothnian Bay sediments we should see an increase in methanogenic rates. We did not notice an increase in methanogenic rates in spiked cultures compared to control cultures (Fig. S6F). This indicates that (exo)cellular enzymes/shuttles are unlikely to play a role in conductive particle-mediated SAO between *Geobacter* and *Methanosarcina*.

Conclusion. Here, we showed that syntrophic acetate oxidation was coupled to CO_2-reductive methanogenesis via conductive particles in mud-free *Desulfuromonadales-Methanosarcina* consortia from the Baltic Sea. Our results suggest that conductive particles are essential for syntrophic acetate oxidation coupled to CO_2-reductive methanogenesis in sediments. Mineral-SAO could have significant implications for the isotopic composition and the cycling of methane in aquatic sediments. Anthropogenic activity could enhance the input of conductive materials to sediments, ultimately increasing methane fluxes. Since methane is a powerful greenhouse gas, we must better understand such actuators of methane emissions in the environment.

MATERIALS AND METHODS

Sampling and incubations. During an expedition on board the RV Fyrbygarrren in July 2014, we sampled sediment cores with a Gemini gravity corer. Three sediment cores were gathered at station RA2,

which is located near the Swedish shoreline (coordinates: 22°26.8′E, 65°43.8′N). Within 24 h after sampling, the sediment was partitioned into depth-profiled aliquots and fixed for biogeochemical and molecular analyses inside an on-deck N_2-inflatable glove bag, as described below in detail.

For incubations, we gathered methanogenic sediment from a depth of 30 to 36 cm and replaced the gas atmosphere with 2×10^5 Pa of N_2-CO_2 (80:20) mix. The 30-to-36-cm-depth sediment was stored at 4°C until we generated slurries with various substrates and minerals.

Slurries were prepared in the lab in an anaerobic chamber and were generated within 6 months after sampling. For slurries, we used 3-ml cut-off syringes to distribute 2.5 ml sediment into 20-ml gas-tight vials with 7.5 ml DSM 120-modified medium. The modified DSM 120 medium was prepared as described before (48) but with 0.6 g NaCl. Sediment slurries had a high organic content, whereas mud-free enrichments did not. Therefore, we amended the mud-free enrichments with 0.2 g/liter yeast extract from a 100-g/liter anaerobic and sterile stock, which is required for methanogenic growth. Before inoculation, the complete medium which lacked the substrate and (semi)conductive minerals was dispensed anaerobically by syringe into sterile degased vials with or without minerals prepared as described below.

Conductive materials, GAC (0.1 g/10 ml; Merck), and magnetite (0.1 g/10 ml; Sigma-Aldrich) were weighed, added to vials, overlaid with 200 μl ultrapure water for wet sterilization, degased for 3 min with an N_2-CO_2 (80:20) mix, and autoclaved at 121°C for 25 min. Control experiments were carried out with acid-washed glass beads instead of conductive minerals. Substrates (5 mM glucose, 5 mM butyrate, 10 mM acetate, 10 mM ethanol) were added to media from sterile anoxic 1 M stocks by aseptic and anaerobic techniques. Control experiments were carried out without additional substrate to learn if the organic compounds in sediment could be used as substrates for methanogenesis. All incubations were carried out at room temperature (20 to 23°C) in triplicate unless otherwise noted.

Gas samples were withdrawn at timed intervals using hypodermic needles connected to a syringe closed by an airtight valve. Gas samples (0.5 ml) were stored, until measured, by displacing 0.5 ml ultrapure water, which filled 3-ml Exetainers. Thirty-microliter gas samples were tested for methane on a Thermo Scientific gas chromatograph equipped with a TG-Bond Msieve 5A column (30 m by 0.53 mm by 50 μm) and a flame ionization detector (FID). The carrier was N_2 (flow rate, 5 ml/min), and we used an isothermal oven temperature of 150°C with the injector and detector set at 200°C. Gas standards (0.01% to 50% CH_4 in N_2) from Mikrolab Aarhus A/S were always run along with samples. Short-chain volatile fatty acids (SCVFA) were detected via high-performance liquid chromatography (HPLC) of 0.45-μm-filtered and 3-times-diluted samples. For HPLC, we used an Agilent 1100 instrument equipped with an Aminex-HPX 87H column heated at 70°C and a VWR detector, which detects SCVFA at 210 nm. Five millimoles of sulfuric acid was used as eluent at a flow rate of 0.6 ml/min. Standards used ranged between 0.1 mM and 10 mM. The detection limit for all SCVFA was 100 μM.

Biogeochemical analyses. To determine biogeochemical parameters, we took sediment aliquots from every 2 cm in an anaerobic glove bag filled with N_2 gas. At this station, the sulfide-methane transition zone was below 15 cm. Geochemical parameters of direct relevance to this work were methane, dissolved inorganic carbon (DIC), and resident iron and manganese oxide species. For *in situ* methane concentrations and $^{13}C/^{12}C$-methane isotopic fractionation, we blocked the activity of the microorganisms by immersing 2 ml active sediment into 4 ml of 2.5% NaOH. NaOH-treated samples kept in gas-tight vials were stored at 4°C, upside down, until methane could be measured.

Methane headspace concentrations were measured on a PerkinElmer gas chromatograph (GC) equipped with an EliteQPlus capillary column with an inner diameter of 0.52 mm heated to 50°C and an FID heated to 200°C. The carrier gas was N_2 with a flow rate of 10 ml/min. $\delta^{13}C_{CH4}$ values were measured at Aarhus University on an isotope-mass ratio gas chromatograph-mass spectrometer as described before (75).

For determination of iron and manganese, 5 ml of sediment was subsampled from each 2-cm-depth interval, transferred into 15-ml centrifugation vials, and stored at −20°C until extraction of the different iron and manganese phases. Three different extraction methods were applied: the cold 0.5 N HCl extraction (to dissolve poorly crystalline iron oxides FeS and $FeCO_3$), the dithionite extraction (to dissolve all the other Fe-oxides except for magnetite), and oxalate extraction (to dissolve magnetite) (68, 73), followed by a ferrozine assay (74). For analysis of manganese, extractions were carried out as described for solid iron, and concentrations in the supernatant were analyzed undiluted by flame atomic absorption spectroscopy.

For pore water parameters, porosity of the sediments was calculated from identifying the relationship between the wet weight of the sediment and its dry weight. For pore water extraction, 50 ml sediment was sampled every 2 cm by scooping sediment into Falcon tubes, from which pore water was extracted with the use of rhizons (rhizosphere; pore size, 0.2 μm). Pore water work was carried out under a N_2 atmosphere in a glove bag.

For pore water Fe^{2+} and Mn^{2+} concentrations, 1 ml pore water was mixed with 20 μl 6 N HCl and stored at −20°C. Soluble Fe^{2+} in the pore water was determined using the ferrozine assay (74).

Pore water DIC was sampled inside an N_2-filled glove bag on board. DIC samples were filled to brim to ensure no gas bubbles into 3-ml glass vials, which contained 20 μl $HgCl_2$-saturated water. Samples were stored upside down at 4°C until measurements. For measurements, we converted DIC to CO_2 by acidification with 50 μl undiluted H_2PO_4 for each 200-μl DIC sample. CO_2 was allowed to equilibrate in the headspace overnight inside 12-ml He-flushed Exetainers. DIC concentration and the $[^{13}C/^{12}C]$DIC isotope ratios were measured on an isotope ratio mass spectrometer coupled to a gas bench, as previously described (75).

Molecular analyses. For molecular analyses, we sampled 2 ml from every 2 cm of sediment depth. Samples were collected using cut-off syringes at the same time with samples for biogeochemical parameters, on board and inside an anaerobic bag. For safe storage during transportation, 3 depths, so a total of 6 cm, were pooled together and mixed with 6 ml MoBio RNAlater (1:1). Prior to DNA extractions, RNAlater was removed by centrifugation. For DNA extraction, we used the MoBio RNA soil kit coupled to a cDNA soil kit and followed the instructions provided by the kit manufacturer. DNA was quantified using a Nano Drop before downstream applications.

Quantitative PCR. To target electrogenic microorganisms, genus/order-specific PCR was performed with primers for *Desulfuromonadales* (includes all *Geobacter*), *Geothrix*, *Rhodoferrax* and *Shewanella*. For methanogens, the following genus/order-specific primers were tested to target: Methanosarcinaceae, *Methanothrix*, Methanococcales, *Methanobacteriales*, Methanomicrobiales. A list of all the primers used, making of standards, and the conditions for quantitative PCR (qPCR) are available in Table S1F and Text S1, respectively.

16S rRNA gene sequencing, library preparation, and phylogenetic tree reconstruction. 16S rRNA gene MiSeq amplicon sequencing was carried out from the 30-to-36-cm-depth interval of triplicate cores. Details on the procedure can be found in Text S1. Qualitative and quantitative information regarding MiSeq sequence reads can be found in Fig. S1 in the supplemental material. Amplification of partial *Geobacter* and *Methanosarcina* 16S rRNA gene sequences was done as described before (76). Cloning employed the TOPO TA cloning kit (Thermo, Fisher Scientific) followed by direct sequencing of PCR products from cloned plasmid DNA (Macrogen). Maximum likelihood phylogenetic trees were constructed using Geneious (77).

^{13}C labeling experiments. Cultures were incubated with a 1:9 mix of $^{13}CH_3COOH$ and unlabeled acetate. Approximatgely 21 cultures with GAC and 16 for the GAC-free cultures were started for the nanoSIMS experiment, because we would sacrificially harvest three at each time point. Headspace gas samples and VFA samples were analyzed as above.

We followed enrichment of $^{13}CO_2$ over time by using IR-MS. Briefly, 2.5-ml media samples were retrieved anaerobically for $^{13}CO_2$ analyses and immediately stored with 20 μl $HgCl_2$-saturated water, without any headspace, and acidified as explained above for DIC analyses in sediment samples; finally, IR-MS analyses were carried out manually against CO_2 gas standards and bicarbonate standards.

We followed the incorporation of labeled acetate ($^{13}CH_3COOH$) into a specific phylotype by using CARD-FISH coupled to nanoSIMS, as described below (78).

CARD-FISH. To count cells of a specific phylogenetic group and label cells prior to nanoSIMS, we used CARD-FISH as described previously (79) and the following probes: Non338 (80) to check for nonspecific binding, Eub338I-III (81, 82) to target *Eubacteria*, Geo3a-c in equimolar amounts with helpers H-Geo3-3 and H-Geo3-4 to target the *Geobacterales* cluster (83); Arch915 (72) to target *Archaea*, and MS821 (72) to target *Methanosarcina* species. A detailed description of the CARD-FISH protocol can be found in Text S1.

Quantitative imaging of ^{13}C label incorporation via nanoSIMS. Chemical imaging and quantitative analysis of ^{13}C label incorporation was carried out on a NanoSIMS-50L instrument (Cameca, Ametek) operating in negative extraction mode. nanoSIMS analyses were carried out on laser microdissection-selected fields, and the collected data were quantitatively analyzed using the LANS software (84). A detailed description of the protocol used for nanoSIMS analyses and data collection can be found in Text S1.

Accession number(s). Sequence files for our partial *Geobacter* and *Methanosarcina* 16S rRNA gene sequences and 16S MiSeq sequence data can be found at NCBI under BioProject ID PRJNA415800.

SUPPLEMENTAL MATERIAL

Supplemental material for this article may be found at https://doi.org/10.1128/mBio.00226-18.

TEXT S1, DOCX file, 0.2 MB.
FIG S1, PDF file, 0.2 MB.
FIG S2, PDF file, 0.04 MB.
FIG S3, PDF file, 0.05 MB.
FIG S4, PDF file, 0.03 MB.
FIG S5, PDF file, 1.2 MB.
FIG S6, PDF file, 0.03 MB.
TABLE S1, DOCX file, 0.1 MB.
TABLE S2, DOCX file, 0.05 MB.

ACKNOWLEDGMENTS

This work is a contribution to Danish Research Council (DFF) grant 1325-00022 to A.-E.R. DFF grant 4181-00203 supported O.S.W. The RV Fyrbyggaren expedition was cofinanced by a Swedish Research Council (VR) grant to Phys A DFF (grant 4002-00521) to B.T.

We acknowledge the Centre for Chemical Microscopy (ProVIS) at the Helmholtz

Centre for Environmental Research supported by the European Regional Development Funds (EFRE—Europe funds Saxony) for use of their analytic facilities. We thank Lasse Ørum Smidt, Heidi Grøn Jensen, Susanne Møller, Erik Laursen, Bente Holbech, Karina Henricksen, Laura Bristow, and Fanghua Liu for help with different aspects of the work and two anonymous reviewers for their helpful feedback.

Author contributions to this study included the following: experimental design by A.-E.R., B.T., and N.M.; sampling by A.E.R., P.O.J.H., and H.S.W.; incubations by A.E.-R.; biogeochemical parameters by A.E.R., P.O.J.H., B.T., and H.S.W.; community analyses by A.-E.R., P.M.S., and O.L.O.S.-W.; stable isotope experiments and analyses by A.-E.R., B.T., and F.M.; CARD-FISH coupled with nanoSIMS experiments and analyses by A.-E.R., F.C., H.S., H.H.R., F.M., and N.M.; manuscript written by A.-E.R. with contribution from all authors.

REFERENCES

1. Hattori S. 2008. Syntrophic acetate-oxidizing microbes in methanogenic environments. Microbes Environ 23:118–127. https://doi.org/10.1264/jsme2.23.118.
2. Galushko AS, Schink B. 2000. Oxidation of acetate through reactions of the citric acid cycle by Geobacter sulfurreducens in pure culture and in syntrophic coculture. Arch Microbiol 174:314–321. https://doi.org/10.1007/s002030000208.
3. Hattori S, Kamagata Y, Hanada S, Shoun H. 2000. Thermacetogenium phaeum gen. nov., sp. nov., a strictly anaerobic, thermophilic, syntrophic acetate-oxidizing bacterium. Int J Syst Evol Microbiol 50:1601–1609. https://doi.org/10.1099/00207713-50-4-1601.
4. Schnurer A, Schink B, Svensson BH. 1996. Clostridium ultunense sp. nov., a mesophilic bacterium oxidizing acetate in syntrophic association with a hydrogenotrophic methanogenic bacterium. Int J Syst Bacteriol 46:1145–1152. https://doi.org/10.1099/00207713-46-4-1145.
5. Balk M, Weijma J, Stams AJM. 2002. Thermotoga lettingae sp. nov., a novel thermophilic, methanol-degrading bacterium isolated from a thermophilic anaerobic reactor. Int J Syst Evol Microbiol 52:1361–1368. https://doi.org/10.1099/00207713-52-4-1361.
6. Westerholm M, Roos S, Schnürer A. 2010. Syntrophaceticus schinkii gen. nov., sp. nov., an anaerobic, syntrophic acetate-oxidizing bacterium isolated from a mesophilic anaerobic filter. FEMS Microbiol Lett 309:100–104. https://doi.org/10.1111/j.1574-6968.2010.02023.x.
7. Zhilina TN, Zavarzina DG, Kolganova TV, Tourova TP, Zavarzin GA. 2005. "Candidatus Contubernalis alkalaceticum," an obligately syntrophic alkaliphilic bacterium capable of anaerobic acetate oxidation in a coculture with *Desulfonatronum cooperativum*. Microbiology 74:695–703. https://doi.org/10.1007/s11021-005-0126-4.
8. Cord-Ruwisch R, Lovley DR, Schink B. 1998. Growth of Geobacter sulfurreducens with acetate in syntrophic cooperation with hydrogen-oxidizing anaerobic partners. Appl Environ Microbiol 64:2232–2236.
9. Kimura Z, Okabe S. 2013. Acetate oxidation by syntrophic association between Geobacter sulfurreducens and a hydrogen-utilizing exoelectrogen. ISME J 7:1472–1482. https://doi.org/10.1038/ismej.2013.40.
10. Wang LY, Nevin KP, Woodard TL, Mu BZ, Lovley DR. 2016. Expanding the diet for DIET: electron donors supporting direct interspecies electron transfer (DIET) in defined co-cultures. Front Microbiol 7:236. https://doi.org/10.3389/fmicb.2016.00236.
11. Galouchko AS, Rozanova EP. 1996. Sulfidogenic oxidation of acetate by a syntrophic association of anaerobic mesophilic bacteria. Microbiology 65:134–139.
12. Tang J, Zhuang L, Ma J, Tang Z, Yu Z, Zhou S. 2016. Secondary mineralization of ferrihydrite affects microbial methanogenesis in Geobacter-Methanosarcina cocultures. Appl Environ Microbiol 82:5869–5877. https://doi.org/10.1128/AEM.01517-16.
13. Zinder SH. 1989. Syntrophic acetate oxidation and "reversible acetogenesis," p 386–415. *In* Drake HL (ed), Acetogenesis. Springer, Boston, MA.
14. Zinder SH, Koch M. 1984. Non-aceticlastic methanogenesis from acetate: acetate oxidation by a thermophilic syntrophic coculture. Arch Microbiol 138:263–272. https://doi.org/10.1007/BF00402133.
15. Phelps TJ, Conrad R, Zeikus JG. 1985. Sulfate-dependent interspecies H_2 transfer between Methanosarcina barkeri and Desulfovibrio vulgaris during coculture metabolism of acetate or methanol. Appl Environ Microbiol 50:589–594.
16. Ozuolmez D, Na H, Lever MA, Kjeldsen KU, Jörgensen BB, Plugge CM. 2015. Methanogenic archaea and sulfate reducing bacteria co-cultured on acetate: teamwork or coexistence? Front Microbiol 6:1–12. https://doi.org/10.3389/fmicb.2015.00492.
17. Petersen SP, Ahring BK. 1991. Acetate oxidation in a thermophilic anaerobic sewage-sludge digestor: the importance of non-aceticlastic methanogenesis from acetate. FEMS Microbiol Lett 86:149–158. https://doi.org/10.1111/j.1574-6968.1991.tb04804.x.
18. Schnurer A, Zellner G, Svensson BH. 1999. Mesophilic syntrophic acetate oxidation during methane formation in biogas reactors. FEMS Microbiol Ecol 29:249–261.
19. Lee SH, Park JH, Kim SH, Yu BJ, Yoon JJ, Park HD. 2015. Evidence of syntrophic acetate oxidation by Spirochaetes during anaerobic methane production. Bioresour Technol 190:543–549. https://doi.org/10.1016/j.biortech.2015.02.066.
20. Angenent LT, Sung S, Raskin L. 2002. Methanogenic population dynamics during startup of a full-scale anaerobic sequencing batch reactor treating swine waste. Water Res 36:4648–4654. https://doi.org/10.1016/S0043-1354(02)00199-9.
21. Karakashev D, Batstone DJ, Trably E, Angelidaki I. 2006. Acetate oxidation is the dominant methanogenic pathway from acetate in the absence of Methanosaetaceae. Appl Environ Microbiol 72:5138–5141. https://doi.org/10.1128/AEM.00489-06.
22. Tatara M, Makiuchi T, Ueno Y, Goto M, Sode K. 2008. Methanogenesis from acetate and propionate by thermophilic down-flow anaerobic packed-bed reactor. Bioresour Technol 99:4786–4795. https://doi.org/10.1016/j.biortech.2007.09.069.
23. Westerholm M, Dolfing J, Sherry A, Gray ND, Head IM, Schnürer A. 2011. Quantification of syntrophic acetate-oxidizing microbial communities in biogas processes. Environ Microbiol Rep 3:500–505. https://doi.org/10.1111/j.1758-2229.2011.00249.x.
24. Ho D, Jensen P, Gutierrez-Zamora ML, Beckmann S, Manefield M, Batstone D. 2016. High-rate, high temperature acetotrophic methanogenesis governed by a three population consortium in anaerobic bioreactors. PLoS One 11:e0159760. https://doi.org/10.1371/journal.pone.0159760.
25. Mosbæk F, Kjeldal H, Mulat DG, Albertsen M, Ward AJ, Feilberg A, Nielsen JL. 2016. Identification of syntrophic acetate-oxidizing bacteria in anaerobic digesters by combined protein-based stable isotope probing and metagenomics. ISME J 10:2405–2418. https://doi.org/10.1038/ismej.2016.39.
26. Müller B, Sun L, Westerholm M, Schnürer A. 2016. Bacterial community composition and fhs profiles of low—and high—ammonia biogas digesters reveal novel syntrophic acetate-oxidising bacteria. Biotechnol Biofuels 9:48. https://doi.org/10.1186/s13068-016-0454-9.
27. Nüsslein B, Chin KJ, Eckert W, Conrad R. 2001. Evidence for anaerobic syntrophic acetate oxidation during methane production in the profundal sediment of subtropical Lake Kinneret (Israel). Environ Microbiol 3:460–470. https://doi.org/10.1046/j.1462-2920.2001.00215.x.
28. Zheng S, Zhang H, Li Y, Zhang H, Wang O, Zhang J, Liu F. 2015. Co-occurrence of Methanosarcina mazei and Geobacteraceae in an iron(III)-reducing enrichment culture. Front Microbiol 6:00941. https://doi.org/10.3389/fmicb.2015.00941.
29. Chauhan A, Ogram A. 2006. Fatty acid-oxidizing consortia along a nutrient gradient in the Florida Everglades. Appl Environ Microbiol 72:2400–2406. https://doi.org/10.1128/AEM.72.4.2400-2406.2006.

30. Hori T, Noll M, Igarashi Y, Friedrich MW, Conrad R. 2007. Identification of acetate-assimilating microorganisms under methanogenic conditions in anoxic rice field soil by comparative stable isotope probing of RNA. Appl Environ Microbiol 73:101–109. https://doi.org/10.1128/AEM.01676-06.
31. Liu F, Conrad R. 2010. Thermoanaerobacteriaceae oxidize acetate in methanogenic rice field soil at 50°C. Environ Microbiol 12:2341–2354. https://doi.org/10.1111/j.1462-2920.2010.02289.x.
32. Rui J, Qiu Q, Lu Y. 2011. Syntrophic acetate oxidation under thermophilic methanogenic conditions in Chinese paddy field soil. FEMS Microbiol Ecol 77:264–273. https://doi.org/10.1111/j.1574-6941.2011.01104.x.
33. Mayumi D, Mochimaru H, Yoshioka H, Sakata S, Maeda H, Miyagawa Y, Ikarashi M, Takeuchi M, Kamagata Y. 2011. Evidence for syntrophic acetate oxidation coupled to hydrogenotrophic methanogenesis in the high-temperature petroleum reservoir of Yabase oil field (Japan). Environ Microbiol 13:1995–2006. https://doi.org/10.1111/j.1462-2920.2010.02338.x.
34. Mark Jensen MM, Thamdrup B, Rysgaard S, Holmer M, Fossing H. 2003. Rates and regulation of microbial iron reduction in sediments of the Baltic-North Sea transition. Biogeochemistry 65:295–317. https://doi.org/10.1023/A:1026261303494.
35. Maher BA, Taylor RM. 1988. Formation of ultrafine-grained magnetite in soils. Nature 336:368–370. https://doi.org/10.1038/336368a0.
36. Nielsen LP, Risgaard-Petersen N, Fossing H, Christensen PB, Sayama M. 2010. Electric currents couple spatially separated biogeochemical processes in marine sediment. Nature 463:1071–1074. https://doi.org/10.1038/nature08790.
37. Liesack W, Schnell S, Revsbech NP. 2000. Microbiology of flooded rice paddies. FEMS Microbiol Rev 24:625–645. https://doi.org/10.1016/S0168-6445(00)00050-4.
38. Schmidt MWI, Noack AG. 2000. Black carbon in soils and sediments: analysis, distribution, implications, and current challenges. Global Biogeochem Cycles 14:777–793. https://doi.org/10.1029/1999GB001208.
39. Middelburg JJ, Nieuwenhuize J, van Breugel P. 1999. Black carbon in marine sediments. Mar Chem 65:245–252. https://doi.org/10.1016/S0304-4203(99)00005-5.
40. Marinho B, Ghislandi M, Tkalya E, Koning CE, de With G. 2012. Electrical conductivity of compacts of graphene, multi-wall carbon nanotubes, carbon black, and graphite powder. Powder Technol 221:351–358. https://doi.org/10.1016/j.powtec.2012.01.024.
41. Liu F, Rotaru AE, Shrestha PM, Malvankar NS, Nevin KP, Lovley DR. 2015. Magnetite compensates for the lack of a pilin-associated c-type cytochrome in extracellular electron exchange. Environ Microbiol 17:648–655. https://doi.org/10.1111/1462-2920.12485.
42. Liu F, Rotaru A, Shrestha PM, Malvankar NS, Nevin KP, Lovley DR. 2012. Promoting direct interspecies electron transfer with activated carbon. Energy Environ Sci 5:8982. https://doi.org/10.1039/c2ee22459c.
43. Chen S, Rotaru AE, Shrestha PM, Malvankar NS, Liu F, Fan W, Nevin KP, Lovley DR. 2014. Promoting interspecies electron transfer with biochar. Sci Rep 4:5019. https://doi.org/10.1038/srep05019.
44. Chen S, Rotaru AE, Liu F, Philips J, Woodard TL, Nevin KP, Lovley DR. 2014. Carbon cloth stimulates direct interspecies electron transfer in syntrophic co-cultures. Bioresour Technol 173:82–86. https://doi.org/10.1016/j.biortech.2014.09.009.
45. Yang Z, Shi X, Wang C, Wang L, Guo R. 2015. Magnetite nanoparticles facilitate methane production from ethanol via acting as electron acceptors. Sci Rep 5:16118. https://doi.org/10.1038/srep16118.
46. Zhuang L, Tang J, Wang Y, Hu M, Zhou S. 2015. Conductive iron oxide minerals accelerate syntrophic cooperation in methanogenic benzoate degradation. J Hazard Mater 293:37–45. https://doi.org/10.1016/j.jhazmat.2015.03.039.
47. Summers ZM, Fogarty HE, Leang C, Franks AE, Malvankar NS, Lovley DR. 2010. Direct exchange of electrons within aggregates of an evolved syntrophic coculture of anaerobic bacteria. Science 330:1413–1415. https://doi.org/10.1126/science.1196526.
48. Rotaru AE, Shrestha PM, Liu F, Markovaite B, Chen S, Nevin KP, Lovley DR. 2014. Direct interspecies electron transfer between Geobacter metallireducens and Methanosarcina barkeri. Appl Environ Microbiol 80:4599–4605. https://doi.org/10.1128/AEM.00895-14.
49. Rotaru A-E, Shrestha PM, Liu F, Shrestha M, Shrestha D, Embree M, Zengler K, Wardman C, Nevin KP, Lovley DR. 2014. A new model for electron flow during anaerobic digestion: direct interspecies electron transfer to Methanosaeta for the reduction of carbon dioxide to methane. Energy Environ Sci 7:408–415. https://doi.org/10.1039/C3EE42189A.
50. Zhao Z, Zhang Y, Woodard TL, Nevin KP, Lovley DR. 2015. Enhancing syntrophic metabolism in up-flow anaerobic sludge blanket reactors with conductive carbon materials. Bioresour Technol 191:140–145. https://doi.org/10.1016/j.biortech.2015.05.007.
51. Xu S, He C, Luo L, Lü F, He P, Cui L. 2015. Comparing activated carbon of different particle sizes on enhancing methane generation in upflow anaerobic digester. Bioresour Technol 196:606–612. https://doi.org/10.1016/j.biortech.2015.08.018.
52. Cruz Viggi C, Rossetti S, Fazi S, Paiano P, Majone M, Aulenta F. 2014. Magnetite particles triggering a faster and more robust syntrophic pathway of methanogenic propionate degradation. Environ Sci Technol 48:7536–7543. https://doi.org/10.1021/es5016789.
53. Li H, Chang J, Liu P, Fu L, Ding D, Lu Y. 2015. Direct interspecies electron transfer accelerates syntrophic oxidation of butyrate in paddy soil enrichments. Environ Microbiol 17:1533–1547. https://doi.org/10.1111/1462-2920.12576.
54. Zhang J, Lu Y. 2016. Conductive Fe3O4 nanoparticles accelerate syntrophic methane production from butyrate oxidation in two different lake sediments. Front Microbiol 7:1316. https://doi.org/10.3389/fmicb.2016.01316.
55. Dolfing J. 2014. Thermodynamic constraints on syntrophic acetate oxidation. Appl Environ Microbiol 80:1539–1541. https://doi.org/10.1128/AEM.03312-13.
56. Kato S, Hashimoto K, Watanabe K. 2012. Microbial interspecies electron transfer via electric currents through conductive minerals. Proc Natl Acad Sci U S A 109:10042–10046. https://doi.org/10.1073/pnas.1117592109.
57. Conrad R, Klose M. 2011. Stable carbon isotope discrimination in rice field soil during acetate turnover by syntrophic acetate oxidation or acetoclastic methanogenesis. Geochim Cosmochim Acta 75:1531–1539. https://doi.org/10.1016/j.gca.2010.12.019.
58. Kastening B, Hahn M, Rabanus B, Heins M, zum Felde U. 1997. Electronic properties and double layer of activated carbon? Electrochim Acta 42:2789–2799. https://doi.org/10.1016/S0013-4686(97)00082-0.
59. Fallas Dotti M. 2015. Origin and evolution of sulfur processing organisms through time. PhD dissertation. University of Southern Denmark, Odense, Denmark.
60. Egger M, Rasigraf O, Sapart CJ, Jilbert T, Jetten MS, Röckmann T, van der Veen C, Bândă N, Kartal B, Ettwig KF, Slomp CP. 2015. Iron-mediated anaerobic oxidation of methane in brackish coastal sediments. Environ Sci Technol 49:277–283. https://doi.org/10.1021/es503663z.
61. Sánchez-García L, Cato I, Gustafsson Ö. 2010. Evaluation of the influence of black carbon on the distribution of PAHs in sediments from along the entire Swedish continental shelf. Mar Chem 119:44–51. https://doi.org/10.1016/j.marchem.2009.12.005.
62. Edlund A, Hårdeman F, Jansson JK, Sjöling S. 2008. Active bacterial community structure along vertical redox gradients in Baltic Sea sediment. Environ Microbiol 10:2051–2063. https://doi.org/10.1111/j.1462-2920.2008.01624.x.
63. Fey A, Claus P, Conrad R. 2004. Temporal change of 13C-isotope signatures and methanogenic pathways in rice field soil incubated anoxically at different temperatures. Geochim Cosmochim Acta 68:293–306. https://doi.org/10.1016/S0016-7037(03)00426-5.
64. Rotaru AE, Woodard TL, Nevin KP, Lovley DR. 2015. Link between capacity for current production and syntrophic growth in Geobacter species. Front Microbiol 6:744. https://doi.org/10.3389/fmicb.2015.00744.
65. Salvador AF, Martins G, Melle-Franco M, Serpa R, Stams AJM, Cavaleiro AJ, Pereira MA, Alves MM. 2017. Carbon nanotubes accelerate methane production in pure cultures of methanogens and in a syntrophic coculture. Environ Microbiol 19:2727–2739. https://doi.org/10.1111/1462-2920.13774.
66. Thauer RK, Kaster AK, Seedorf H, Buckel W, Hedderich R. 2008. Methanogenic archaea: ecologically relevant differences in energy conservation. Nat Rev Microbiol 6:579–591. https://doi.org/10.1038/nrmicro1931.
67. Roden EE, Zachara JM. 1996. Microbial reduction of crystalline iron (III) oxides: influence of oxide surface area and potential for cell growth. Environ Sci Technol 30:1618–1628. https://doi.org/10.1021/es9506216.
68. Kostka JE, Luther GW. 1994. Partitioning and speciation of solid phase iron in saltmarsh sediments. Geochim Cosmochim Acta 58:1701–1710. https://doi.org/10.1016/0016-7037(94)90531-2.
69. Van Bodegom PM, Scholten JCM, Stams AJM. 2004. Direct inhibition of methanogenesis by ferric iron. FEMS Microbiol Ecol 49:261–268. https://doi.org/10.1016/j.femsec.2004.03.017.
70. Summers ZM, Gralnick JA, Bond DR. 2013. Cultivation of an obligate Fe(II)-oxidizing lithoautotrophic bacterium using electrodes. mBio 4:e00420-12. https://doi.org/10.1128/mBio.00420-12.

71. Deutzmann JS, Sahin M, Spormann AM. 2015. Extracellular enzymes facilitate electron uptake in biocorrosion and bioelectrosynthesis. mBio 6:e00496-15. https://doi.org/10.1128/mBio.00496-15.
72. Raskin L, Stromley JM, Rittmann BE, Stahl DA. 1994. Group-specific 16S rRNA hybridization probes to describe natural communities of methanogens. Appl Environ Microbiol 60:1232–1240.
73. Thamdrup B, Fossing H, Jørgensen BB. 1994. Manganese, iron and sulfur cycling in a coastal marine sediment, Aarhus Bay, Denmark. Geochim Cosmochim Acta 58:5115–5129. https://doi.org/10.1016/0016-7037(94)90298-4.
74. Lovley DR, Phillips EJP. 1987. Rapid assay for microbially reducible ferric iron in aquatic sediments. Appl Environ Microbiol 53:1536–1540.
75. Norði Kà, Thamdrup B, Schubert CJ. 2013. Anaerobic oxidation of methane in an iron-rich Danish freshwater lake sediment. Limnol Oceanogr 58:546–554. https://doi.org/10.4319/lo.2013.58.2.0546.
76. Snoeyenbos-West OL, Nevin KP, Anderson RT, Lovley DR. 2000. Enrichment of Geobacter species in response to stimulation of Fe(III) reduction in sandy aquifer sediments. Microb Ecol 39:153–167. https://doi.org/10.1007/s002480000018.
77. Kearse M, Moir R, Wilson A, Stones-Havas S, Cheung M, Sturrock S, Buxton S, Cooper A, Markowitz S, Duran C, Thierer T, Ashton B, Meintjes P, Drummond A. 2012. Geneious Basic: an integrated and extendable desktop software platform for the organization and analysis of sequence data. Bioinformatics 28:1647–1649. https://doi.org/10.1093/bioinformatics/bts199.
78. Musat N, Halm H, Winterholler B, Hoppe P, Peduzzi S, Hillion F, Horreard F, Amann R, Jørgensen BB, Kuypers MM. 2008. A single-cell view on the ecophysiology of anaerobic phototrophic bacteria. Proc Natl Acad Sci U S A 105:17861–17866. https://doi.org/10.1073/pnas.0809329105.
79. Pernthaler J, Glöckner FO, Schönhuber W, Amann R. 2001. Fluorescence in situ hybridization with rRNA-targeted oligonucleotide probes. Methods Microbiol 30:1–31.
80. Wallner G, Amann R, Beisker W. 1993. Optimizing fluorescent in situ hybridization with rRNA-targeted oligonucleotide probes for flow cytometric identification of microorganisms. Cytometry 14:136–143. https://doi.org/10.1002/cyto.990140205.
81. Amann RI, Binder BJ, Olson RJ, Chisholm SW, Devereux R, Stahl DA. 1990. Combination of 16S rRNA-targeted oligonucleotide probes with flow cytometry for analyzing mixed microbial populations. Appl Environ Microbiol 56:1919–1925.
82. Daims H, Brühl A, Amann R, Schleifer KH, Wagner M. 1999. The domain-specific probe EUB338 is insufficient for the detection of all Bacteria: development and evaluation of a more comprehensive probe set. Syst Appl Microbiol 22:434–444. https://doi.org/10.1016/S0723-2020(99)80053-8.
83. Richter H, Lanthier M, Nevin KP, Lovley DR. 2007. Lack of electricity production by Pelobacter carbinolicus indicates that the capacity for Fe(III) oxide reduction does not necessarily confer electron transfer ability to fuel cell anodes. Appl Environ Microbiol 73:5347–5353. https://doi.org/10.1128/AEM.00804-07.
84. Polerecky L, Adam B, Milucka J, Musat N, Vagner T, Kuypers MM. 2012. Look@NanoSIMS —a tool for the analysis of NanoSIMS data in environmental microbiology. Environ Microbiol 14:1009–1023. https://doi.org/10.1111/j.1462-2920.2011.02681.x.
85. Games L, Hayes JM. 1978. Methane-producing bacteria: natural fractionations of the stable carbon isotopes. Geochim Cosmochim Acta 42:1295–1297.
86. Krzycki J, Kenealy W, DeNiro M, Zeikus JG. 1987. Stable carbon isotope fractionation by *Methanosarcina barkeri* during methanogenesis from acetate, methanol, or carbon dioxide-hydrogen. Appl Environ Microbiol 53:2597–2599.
87. Gelwicks JT, Risatti JB, Hayes JM. 1994. Carbon isotope effects associated with aceticlastic methanogenesis. 60:467–472.
88. Lever MA. 2012. Acetogenesis in the energy-starved deep biosphere-a paradox? Front Microbiol 2:284. https://doi.org/10.3389/fmicb.2011.00284.
89. Roden EE, Wetzel RG. 2003. Competition between Fe(III)-reducing and methanogenic bacteria for acetate in iron-rich freshwater sediments. Microb Ecol 45:252–258.
90. Finke N, Vandieken V, Jørgensen BB. 2007. Acetate, lactate, propionate, and isobutyrate as electron donors for iron and sulfate reduction in Arctic marine sediments, Svalbard. FEMS Microbiol Ecol 59:10–22. https://doi.org/10.1111/j.1574-6941.2006.00214.x.